

DMD#9969

Evaluation of time-dependent cytochrome P450 inhibition using cultured human hepatocytes

Dermot F. McGinnity*, Amanda J. Berry, Jane R. Kenny, Ken Grime and Robert J. Riley

Department of Physical & Metabolic Science, AstraZeneca R&D Charnwood, Bakewell Road, Loughborough, Leicestershire. LE11 5RH. U.K.

Running Title

Time-dependent P450 inhibition using cultured hepatocytes

Corresponding Author

Dr. Dermot McGinnity, Department of Physical & Metabolic Science, AstraZeneca R&D Charnwood, Bakewell Road, Loughborough, Leicestershire. LE11 5RH. U.K. Telephone (01509) 644261. Fax (01509) 645576.

E.mail: dermot.f.mcginnity@astrazeneca.com

37 text pages

2 Tables

6 Figures

46 Refs

250 words in Abstract

659 words in Introduction

2264 words in Discussion

Abbreviations

cytochrome P450 (CYP), intrinsic clearance (CL_{int}), metabolic clearance (CL_{met}), mass spectroscopy (MS), unbound fraction in incubation ($f_{u,inc}$), unbound fraction in plasma ($f_{u,p}$), human serum albumin (HSA), bovine serum albumin (BSA), inhibitor concentration ($[I]$), inhibition constant (K_i), CYP degradation or turnover rate constant (k_{deg}), maximal inactivation rate constant (k_{inact}), area under the plasma concentration time curve (AUC), drug-drug interactions (DDIs), hepatocyte maintenance media (HMM).

Abstract

Primary human hepatocytes in culture are commonly used to evaluate CYP induction via an enzyme activity endpoint. However, other processes can confound data interpretation. To this end, the impact of time-dependent CYP inhibition in this system was evaluated. Using a substrate-cassette approach, CYP activities were determined after incubation with the prototypic inhibitors tienilic acid (CYP2C9) and erythromycin, troleandomycin and fluoxetine (CYP3A4). Kinetic analysis of enzyme inactivation in hepatocytes was used to describe the effect of these time-dependent inhibitors and derive the inhibition parameters k_{inact} and K_i , which generally were in good agreement with the values derived using rCYPs and HLM. Tienilic acid selectively inhibited CYP2C9 dependent diclofenac 4'-hydroxylation activity and erythromycin, troleandomycin and fluoxetine inhibited CYP3A4 dependent midazolam 1'-hydroxylation in a time- and concentration-dependent manner. Fluoxetine also inhibited CYP2C9 dependent S-mephenytoin 4'-hydroxylation in a time- and concentration-dependent manner in hepatocytes, HLM and rCYP2C9 (K_i 0.4 μM and k_{inact} 0.5 min^{-1}). As expected, the effect of fluoxetine on CYP2D6 in hepatocytes was consistent with potent yet reversible inhibition. A very weak time-dependent CYP2C9 inhibitor (AZ1, K_i 30 μM & k_{inact} 0.02 min^{-1}) effectively abolished CYP2C9 activity over 24 h at low (μM) concentrations in primary cultured human hepatocytes. This work demonstrates that caution is warranted in the interpretation of enzyme induction studies with metabolically stable, weak time-dependent inhibitors, which may have dramatic inhibitory effects on CYP activity in this system. Therefore, in addition to enzyme activity, mRNA and/or protein levels should be measured in order to fully evaluate the CYP induction potential of a drug candidate.

DMD#9969

Inhibition of cytochrome P450 (CYP) dependent metabolism is a prevalent source of drug-drug interactions (DDIs) and may result in serious clinical consequences (Bertz and Granneman, 1997; Jankel and Fitterman, 1993) via either reversible or irreversible means. An assessment of the potential of a new chemical entity to cause DDIs via inhibition of CYP metabolism is important early in the drug discovery process. Mechanism-based CYP inhibitors can be characterised as displaying NADPH-, concentration- and time-dependent quasi-irreversible or irreversible inactivation due to chemical modification of the heme and/or protein and the inactivation rate is diminished in the presence of a competing substrate (Silverman, 1998). Such inhibitors may be of specific concern; firstly as the *in vivo* inhibitory effect lasts longer than for reversible inhibitors and inactivated CYP has to be replaced by newly synthesised protein; secondly due to an increased toxicological risk via the generation of reactive species (Zhou et al., 2005).

Many drugs are mechanism-based inhibitors of CYP including the macrolide antibiotics erythromycin and troleandomycin (Larrey et al., 1983), tienilic acid (Lopez-Garcia et al., 1994) and fluoxetine (Mayhew et al., 2000). Thus, *in vitro* screens to determine both the degree and nature of CYP inhibition (typically determining the time-dependency of inhibition) are now employed across the pharmaceutical industry. More often than not, these assays focus on the five major drug metabolising CYPs in human: 1A2, 2C9, 2C19, 2D6 and 3A4 and are studied using one or a combination of the following tools; recombinantly expressed CYPs, human liver microsomes and human hepatocytes.

Arguably, human hepatocytes provide the closest *in vitro* model to human liver by providing the full complement of xenobiotic metabolising enzymes and transporters. With the improvement of cryopreservation techniques, human hepatocytes are increasingly used throughout the industry for assessing the metabolic stability of new chemical entities (McGinnity et al., 2004) and more recently for the study of both reversible inhibition of CYP2C9 (McGinnity et al., 2005) and time-dependent inhibition of CYP3A4 (Zhao et al., 2005; Ring et al., 2005). Hepatocytes in primary culture are widely recognised as being the gold standard for predicting CYP induction in both preclinical species and human (Kato

DMD#9969

et al., 2005; Luo et al., 2004; LeCluyse et al., 2000). Induction of CYPs can be demonstrated using one or more of a combination of different endpoints; CYP mRNA, CYP protein via Western blotting and activity using a selective substrate. Although regulation of CYP activity *in vivo* is the key parameter with respect to DDIs, caution must be used when interpreting data from primary cultures based solely on an *in vitro* activity readout since it is recognised that mechanism-based inhibitors of CYPs may lead to a decrease in activity which will be independent of any increase in activity caused by induction (Pichard et al., 1990; Silva and Nicoll-Griffith, 2002; Ring et al., 2005).

The efficiency of time-dependent inhibition is a function of the ratio of k_{inact} (maximal inactivation rate constant) to K_i (inhibitor concentration that supports half the maximal rate of inactivation) both of which can be determined from *in vitro* experiments. Approaches to predicting the *in vivo* DDI potential of time-dependent CYP inhibitors have ranged from a relatively simplistic approach using k_{inact} and K_i values, the enzyme degradation rate (k_{deg}) and a single inhibitor concentration (Mayhew et al., 2000; Wang et al., 2004) to a more complex, physiological based model, incorporating the changing concentrations of inhibitor and substrate (Ito et al., 2003).

In this study, the impact of time-dependent CYP inhibition in human hepatocytes in primary culture has been evaluated, using a substrate cassette strategy. An adaptation of the physiological based model developed by Ito et al., 2003 was used to describe the effect on CYP activities observed in primary culture by prototypic time-dependent CYP inhibitors. K_i and k_{inact} values determined in cultured human hepatocytes were compared with values obtained from rCYPs and HLMs. The additional value of using primary hepatocytes for the assessment of co-incidental time-dependent inhibition and CYP induction is also developed and discussed.

Materials and Methods

Materials

Diclofenac, 4'-hydroxydiclofenac, (\pm)fluoxetine, phenacetin, paracetamol and β -nicotinamide adenine dinucleotide phosphate reduced form (β -NADPH), phosphate buffered saline (PBS) tablets and Tween-20 were purchased from Sigma-Aldrich Chemical (Gillingham, UK) and were of the highest grade available. Bufuralol, S-mephenytoin and midazolam were purchased from Sequoia Research Products Ltd. (Oxford, UK). Hydroxybufuralol, 4'-hydroxymephenytoin and 1'-hydroxymidazolam were purchased from Ultrafine Chemicals (Manchester, UK). Dimethylsulfoxide (DMSO) and trichloroacetic acid were purchased from Fisher Scientific (Loughborough, UK) and methanol was purchased from Romil Ltd. (Cambridge, UK). Hepatocyte maintenance media (HMM) and HMM SingleQuot supplement containing dexamethasone (final concentration 50 nM), gentamicin (50 μ g/ml) and amphotericin B (50 ng/ml) were obtained from Cambrex Bioscience (Wokingham, UK), ITS+ supplement containing insulin (final concentration 6.25 μ g/ml), transferrin (6.25 μ g/ml), selenium (6.25 ng/ml), linoleic acid (5.35 μ g/ml) and bovine serum albumin (1.25 mg/ml), and Sterile 6 well Biocoat® Collagen type I plates were obtained from BD Biosciences (Oxford, UK).

Bactosomes prepared from *E.coli* cells co-expressing recombinant human NADPH-P450 reductase and individual human CYPs (CYP1A2, 2C9, 2C19, 2D6 and 3A4) were purchased from Cypex (Dundee, UK). Pooled human liver microsomes were purchased from BD Gentest (Bedford, MA).

Preparation of Human Hepatocytes

Human hepatocytes were prepared from an isolated lobe of human liver (obtained from local hospitals with ethical approval) using a procedure previously described (McGinnity et al., 2004). Donor demographics for the five hepatocyte donors were as follows: two Caucasian males age 63 and 70 years and three Caucasian females age 64 – 81 years, liver was obtained via surgical resection, medical history not available. Hepatocyte viability

for the five donors, as determined by the trypan blue exclusion method, was between 86-98%.

Culturing of Human Hepatocytes

Freshly isolated hepatocytes were diluted to a cell concentration of approximately 8 million/ml using ice-cold hepatocyte suspension buffer (2.2 g NaHCO₃, 2.34 g Na HEPES, 1 L powder equivalent of DMEM (Sigma, Gillingham, UK) diluted in 1 L of water and adjusted to pH 7.4 with 1 M HCl). Cells were centrifuged (50 g; 5 min; 4 °C), the supernatant removed by aspiration and the pellet resuspended in a small volume of sterile supplemented HMM, counted using the Trypan Blue exclusion method then further diluted to 0.75 million cells per ml. Working using sterile techniques, cells were plated at a seeding density of 1.5 million per well in 2 ml (0.16 million cells/cm²) and left for 16 h at 37°C, 90% relative humidity and 5% CO₂ atmosphere. Cells were washed and assays performed using supplemented HMM.

Determination of CYP activity and CL_{int} of inhibitors in cultured human hepatocytes

Inhibitor and substrate stocks were prepared in DMSO at 200-fold incubation concentrations. To minimise the known CYP inhibitory effects of DMSO, the final concentration in all incubations was 1% (v/v). To cultured human hepatocytes on 6-well collagen coated plates, each 200 x inhibitor stock (10 µl) was added to a well containing supplemented HMM (2 ml) to give final inhibitor concentrations of 0.1, 1 & 10 µM per well. The three remaining wells from each plate were spiked with DMSO (10 µl) as controls. A separate plate was prepared in this way for each time point and inhibitor. At several time points from 0 to 48 h, 200x cassetted substrate stock (10 µl) was added to each well to give a final phenacetin concentration of 26 µM, diclofenac (9 µM), S-mephenytoin (31 µM), bufuralol (9 µM) and midazolam (3 µM). Aliquots (100 µl) were removed 5, 10, 15, 20 and 30 min after addition of probe substrate, and samples quenched in ice-cold methanol (100

DMD#9969

μl). Phenacetin deethylation, diclofenac 4'-hydroxylation, S-mephenytoin 4'-hydroxylation, bufuralol 1'-hydroxylation and midazolam 1'-hydroxylation were used as selective probe reactions for CYP1A2, 2C9, 2C19, 2D6 and 3A4 activity respectively. The CYP isoform selectivity of these reactions have been established previously (Weaver et al., 2003). All substrates were incubated at their measured K_m for the relevant CYP with the exception of diclofenac/CYP2C9 which was incubated at 4 x K_m to allow analytical detection of the metabolite. The formation of 4'-hydroxydiclofenac remains selective for CYP2C9 at 9 μM diclofenac (data not shown). Aliquots from each well were assayed against a metabolite standard curve for the amount of metabolite produced at each time point. The apparent rate of metabolite formation over time was compared in the presence and absence of inhibitor. CYP activity is expressed as a percentage relative to a solvent control incubation (in the absence of inhibitor) at each corresponding time point.

The initial CL_{int} of each inhibitor in cultured human hepatocytes was established on a separate plate using a single, low substrate concentration (1 μM final concentration; 1% (v/v) DMSO). Aliquots (100 μl) were removed at 0, 5, 10, 20, 30, 60 and 90 min and quenched in ice-cold methanol (100 μl). Additionally, to determine the concentration of inhibitor present in the incubation during the assessment of CYP activity (up to 48 h), an aliquot (100 μl) was taken from each well and quenched in ice-cold methanol (100 μl), prior to addition of cassetted substrate.

Samples were subsequently chilled (-20 °C; 1 h) and then centrifuged (3500 rpm; 15 min; 4 °C). The supernatants were removed and transferred into HPLC vials and analysed by HPLC-MS/MS as described below. Cells were collected from the several time point samples and stored (-30 °C) in phosphate buffer (0.1 M; pH 7.4) for Western Blotting.

Estimation of $f_{u,inc}$ in rCYP2C9, human liver microsomes and human hepatocytes

The extent of binding of compounds to rCYP2C9, human liver microsomes and human hepatocytes was estimated using algorithms based on lipophilicity proposed by Austin et al., 2002, 2005.

Determination of K_i & k_{inact} in rCYPs and human liver microsomes

K_i & k_{inact} values were determined in rCYPs and human liver microsomes by an adapted version of the automated method described by Atkinson et al., 2005. Briefly, the pre-incubation used rCYP (25 pmol/ml) or HLM (1 mg/ml) in phosphate buffered saline (0.1 M; pH 7.4), NADPH (1 mM) and six different concentrations of test inhibitor in DMSO (1% v/v) which were incubated at 37°C for 3, 6 and 9 min. Following a ten-fold dilution into NADPH (1 mM) and the relevant CYP substrate, the second reaction was allowed to proceed (15 min). For CYP1A2, phenacetin was used at 75 μ M, 2C9 - diclofenac (10 μ M), 2C19 - S-mephenytoin (100 μ M), 2D6 - bufuralol (40 μ M) and 3A4 - midazolam (10 μ M). Aliquots (50 μ l) were quenched in ice-cold methanol (100 μ l) and prepared for HPLC-MS/MS as described below. Manual incubations were performed for fluoxetine using the method of Atkinson et al., 2005. Briefly, six concentrations (0.04–2 μ M) of fluoxetine in DMSO (1% v/v) were incubated with rCYP (25 pmol/ml) or HLM (1 mg/ml) in phosphate buffered saline (0.1 M; pH 7.4), NADPH (1 mM) at 37°C for 0, 0.5, 1, 2.5, 5 and 10 min. Following a ten-fold dilution into NADPH (1 mM) and S-mephenytoin (100 μ M), the reaction was allowed to proceed (15 min). Aliquots (50 μ l) were quenched in ice-cold methanol (100 μ l) and prepared for HPLC-MS/MS as described below.

Analytical methods

Aliquots (20 μ l) were analysed by HPLC-MS/MS for metabolite appearance of the probes of CYP1A2, 2C9, 2C19, 2D6 and 3A4 activity and parent loss of the inhibitors. Mass spectrometry was conducted on a Micromass Quattro Ultima triple quadrupole by using an Alliance HT Waters 2790 HPLC system for separation. MS conditions for the five metabolites used as probes of CYP activity were as described previously (Weaver et al., 2003). A Synergi (4 μ m) Max-RP C12 column (50 x 4.6 mm, Phenomenex, Cheshire, UK) and mobile phases of 0.1% formic acid in water (A) and 0.1% formic acid in methanol (B)

were used for the chromatography. The gradient was as follows 97% A (0-0.3 min), 5% A (0.55-1.55 min), 97% A (1.6 min). The stop time was 2.5 min, the flow rate was 1.5 ml.min⁻¹ and column temperature 40°C.

Data Analysis

CL_{int} estimates were determined using the rate of parent disappearance (at a single, low substrate concentration) as previously described (McGinnity et al., 2004).

K_i and k_{inact} values in rCYP and HLM were estimated from the natural log of the percent control activity remaining, following incubation with a single inhibitor concentration, plotted against the time of pre-incubation. The slope, k, is the inactivation rate constant (describing the rate of inactivation at that inhibitor concentration). This was determined for data from all inhibitor concentrations. Non-linear regression analysis (WinNonlin™, Pharsight Corporation, North Carolina, USA) was used to determine K_i and k_{inact} from the function:

$$k = \frac{k_{inact} \cdot I}{K_i + I} \quad (1)$$

Where I is the pre-incubation inhibitor concentration, k is the inactivation rate constant for a given I, k_{inact} is the maximal inactivation rate constant and K_i is the inhibitor concentration, I, when the inactivation rate constant is half k_{inact}.

K_i and k_{inact} values were estimated from non-linear regression analysis of the cultured human hepatocyte data (inhibitor concentration and active CYP concentration, E_{act}, at each sampling time point and intrinsic clearance, CL_{int}, of inhibitor). For the mathematical modelling, E₀ (the initial uninhibited CYP concentration) was given the nominal value of 100 (100% active enzyme) and values for E_{act} were likewise expressed as percentages of initial CYP activity. The differential equations were derived from simple relationships describing the clearance of inhibitor and E_{act} from the system (human hepatocytes). In

pharmacokinetics, the clearance of a given parameter is equal to the amount given to the system divided by the total exposure of the system to the parameter. Differentiation of this function reveals that the rate of change of a small amount of the parameter is equal to its clearance multiplied by its concentration at that instant. It follows, therefore, that the rate of change of inhibitor concentration (the rate of change of amount of inhibitor divided by the incubation volume, V_{inc}) in the human hepatocytes is equal to the product of unbound inhibitor CL_{int} and unbound inhibitor concentration, I_u :

$$dI/dt = -((CL_{int} / f_{u_{inc}}) \times I_u \times e^{K.t}) / V_{inc} \quad (2)$$

where $f_{u_{inc}}$ denotes the fraction of inhibitor unbound in the incubation (estimated using the algorithm based on the logP or logD_{7.4} of the inhibitor (Austin et al., 2005). The $f_{u_{inc}}$ values used were 0.1, 1, 0.52, 0.62 and 1 for fluoxetine, tienilic acid, erythromycin, troleandomycin and AZ1 respectively. The unbound inhibitor concentrations (I_u) at each time point were calculated from the measured total inhibitor concentration and $f_{u_{inc}}$. CL_{int} values for each of the test inhibitors were calculated from the respective metabolic half-lives in the plated hepatocyte incubations. When the log observed inhibitor concentrations were not linear with respect to time, CL_{int} values were determined only from the linear portion of the log inhibitor concentration-time profile. Use of these observed CL_{int} values in the model would have resulted in an under-estimation of inhibitor concentration at the later time points, since CL_{int} abated with time. In order to ensure equivalent simulated and observed inhibitor concentrations and therefore ensure accurate I_u values to input into equation 4, an exponential term, $\exp^{K.t}$, was used. Describing equation 2 in this way was necessary because actual inhibitor concentrations were measured only at specified time points, whereas the model requires details of the constantly changing inhibitor concentration so that the continuous alteration of active CYP concentration is conveyed. The constant, K, was determined as follows:

$$K = \text{slope } (0 - t). \frac{\ln ([I]^t \text{ projected from } CL_{\text{int}}^{\text{initial}} / [I]^t \text{ measured})}{t} \quad (3)$$

where $CL_{\text{int}}^{\text{initial}}$ was the CL_{int} established from the linear portion of the log [inhibitor]-time profile and t was every time point at which the inhibitor concentration was determined. The values for K used in the non-linear regression to estimate K_i and k_{inact} were -0.006 for fluoxetine and tienilic acid, -0.002 for erythromycin and 0 for troleandomycin and AZ1. The merit of using these values in the model was assessed by goodness of fit measurements for E_{act} (Akaike criteria and value and spread of residuals).

The rate of change of E_{act} is similarly expressed (equation 4) but takes account of the re-synthesis of active CYP. The clearance of E_{act} in the kinetic model equals the sum of E_{act} entering (synthesis) and leaving (inactivation) the compartment. As with equation 2, a rate of change of concentration rather than amount is described, but no incubation volume term appears because the clearance is written as a sum of rate constants (the rate constant for time dependent inactivation being $k_{\text{inact}} \times I / (K_i + I)$ where clearance equals the product of rate constant and volume. It is also important to note that $E_0 - E_{\text{act}}$, rather than E_{act} , is the “missing” concentration of active CYP driving the resynthesis:

$$dE_{\text{act}} / dt = -(k_{\text{inact}} \times E_{\text{act}} \times I_u / K_i + I_u) + k_{\text{deg}} \times E_0 - E_{\text{act}} \quad (4)$$

where k_{inact} , K_i , E_0 , k_{deg} and $f_{\text{u,inc}}$ represent the maximal inactivation rate constant, the inhibitor concentration when the inactivation rate constant is $k_{\text{inact}}/2$, the initial concentration of CYP and the degradation or turnover rate constant of the inhibited CYP. In the absence of definitive degradation rate constants for individual CYPs in cultured human hepatocytes, unless stated, a value of 0.00025 min^{-1} was used for all CYPs, based on the turnover rate constant for CYP3A in cultured human hepatocytes (Pichard et al., 1992). In the mathematical model described here, it was assumed that the degradation

and synthesis rate constants were equal and that this was unaffected by the presence of CYP inhibitors.

E_{act} values were determined using the CYP-selective probe substrates (CYP2C9-dependant diclofenac 4'-hydroxylation, CYP2C19 S-mephenytoin 4'-hydroxylation, CYP2D6 bufuralol 1'-hydroxylation and CYP3A4 midazolam 1'-hydroxylation) but were modelled as percentages of E_o . Equations (2) and (4) were replicated for each additional concentration of inhibitor used (for example, four differential equations were used to model the data and estimate K_i and k_{inact} when two inhibitor concentrations were used).

In vivo simulation of CYP activity after dosing with AZ1

Using the methodology of Ito et al., 2003 and based on expected human pharmacokinetics and therapeutic dose, CYP2C9 activity in human liver was simulated after oral dosing with AZ1 (70 mg every 24 h for 72 h). Dose 200 μmol ; V_{max} 65 $\mu\text{mol}\cdot\text{min}^{-1}$; k_m 50 μM ; K_{p1} (liver to blood concentration of AZ1) 1; f_b (unbound fraction of AZ1 in blood) 0.01; k_a (first-order absorption rate constant) 0.01 min^{-1} ; F_a (fraction absorbed from gastrointestinal tract) 1; F_g (intestinal availability) 1; V_{sys} volume of distribution in the central compartment 14000 ml; CL_r (renal clearance) 0; CYP2C9 K_i 30 μM and k_{inact} 0.02 min^{-1} .

Results

Determination of inhibitor CL_{int} and CYP activity in cultured human hepatocytes

Estimates of CL_{int} for the CYP inhibitors, tienilic acid, erythromycin, troleandomycin, fluoxetine and a proprietary AstraZeneca compound (AZ1) were determined in cultured human hepatocytes from five individual donors (Table 1). Assays were carried out 12-16 h after plating and CL_{int} values determined by the rate of parent disappearance over 90 min. The activity of the five major human hepatic CYPs (CYP1A2, 2C9, 2C19, 2D6 and 3A4) was assessed in cultured human hepatocytes by use of a cocktail of CYP specific substrates, which allowed for the maximum amount of data to be retrieved from the limited resource of human hepatocytes.

Time-dependent inhibition of CYP activity in cultured human hepatocytes

The limited number of hepatocytes from each individual donor constrained the design of the time course assays. Each inhibitor was incubated with hepatocytes from a minimum of three individual donors over a 48 h time course. The absolute activity in the absence of inhibitor, for the major isoforms studied, CYP2C9 and CYP3A4, changed less than two-fold during the course of the 48 h incubation. To control for these changes in activity over the time course of the experiment, CYP activity was expressed as a % relative to a solvent control at each time point. Using mean CL_{int} and % CYP activity values determined from the human hepatocytes and a CYP turnover constant (k_{deg}) of 0.00025 min^{-1} , as determined for CYP3A4 in cultured human hepatocytes (Pichard et al., 1992) the mean K_i and k_{inact} values were estimated from non-linear regression analysis using Equations 2 and 4.

Fitted inactivation curves for the different concentrations of inhibitors against the individual CYP are compared to the experimental data in Figures 1, 2, 3 and 4.

Figure 1 A, B and C shows mean CYP activities in cultured human hepatocytes over time after incubation with prototypic mechanism based inhibitors tienilic acid, erythromycin and

DMD#9969

troleandomycin respectively. Tienilic acid inhibited CYP2C9 mediated diclofenac 4'-hydroxylation in a time and concentration dependent manner (Figure 1A). During incubation with 1 μM tienilic acid, maximal inhibition (to 5% of control activity) was reached at 9 h post-incubation and this degree of inhibition was maintained for at least 48 h. Tienilic acid at 10 μM effectively abolished CYP2C9 activity for the duration of the experiment. The activities of CYP1A2, 2C19, 2D6 and 3A4 were unaffected by the presence of up to 10 μM tienilic acid. Erythromycin inhibited CYP3A4 mediated midazolam 1'-hydroxylation in a time and concentration dependent manner (Figure 1B). After 5 h incubation, erythromycin at 1 and 10 μM caused maximal CYP3A4 inhibition (to 46 and 10% control activity respectively) and by 48 h, 100 and 59% activity was restored respectively. The activities of CYP1A2, 2C9, 2C19 and 2D6 were unaffected by the presence of up to 10 μM erythromycin. Maximal CYP3A4 inhibition (to 17% of control activity) was reached approximately 5 h into an incubation with 1 μM troleandomycin (Figure 1C), whilst at 10 μM , CYP3A4 activity was effectively abolished by 0.5 h, an inhibition level maintained up to 9 h. Full CYP3A4 activity for both concentrations was restored by 48 h. The activities of CYP1A2, 2C9, 2C19 and 2D6 were unaffected by the presence of up to 10 μM troleandomycin. Mean inhibitor concentrations throughout the time-course of the assay were determined (Figures 1D, E, F). Troleandomycin was essentially cleared after approximately 3 h (Figure 1F), whereas measurable levels of tienilic acid and erythromycin were maintained for the duration of the incubation (Figures 1D, E).

Figure 2 shows the effect of using different k_{deg} values in equation 4 by plotting CYP3A4 activity against time of incubation with troleandomycin with fitted inactivation curves based on using k_{deg} values of A. 0.00025 min^{-1} ($t_{1/2} = 46 \text{ h}$), B. 0.0005 min^{-1} ($t_{1/2} = 23 \text{ h}$) and C. 0.00075 min^{-1} ($t_{1/2} = 15 \text{ h}$). Clearly the rate of regain of activity is a function of k_{deg} , yet over the range used, k_{deg} has little effect on the estimates of K_i and k_{inact} (data not shown).

DMD#9969

Figures 3A, B and C show plots of CYP3A4, 2C19 and 2D6 activity against time of incubation with fluoxetine respectively. Fluoxetine clearly inhibited CYP3A4 mediated midazolam 1'-hydroxylation and CYP2C19 mediated S-mephenytoin 4'-hydroxylation in a time- and concentration-dependent manner. Figure 3A shows CYP3A4 activity was not significantly inhibited by 1 μ M fluoxetine yet reached maximal inhibition 48 h after incubation with 10 μ M fluoxetine (to 31% of control activity). Figure 3B shows CYP2C19 activity was maximally inhibited (to 18% of control activity) between 24-29 h during incubation with 1 μ M fluoxetine and 66% activity was restored by 48 h. Fluoxetine at 10 μ M effectively abolished CYP2C19 activity by 6 h with 38% activity being restored by 48 h. CYP2D6 mediated bufuralol 1'-hydroxylation was inhibited to approximately 60 and 25% of control activity by 1 and 10 μ M fluoxetine respectively (Figure 3C). After 48 h incubation, CYP2D6 activity was reduced to 48 and 16% of control activity by 1 and 10 μ M fluoxetine respectively. CYP1A2 and 2C9 activities were unaffected by the presence of up to 10 μ M fluoxetine. Fluoxetine concentration was determined throughout the time-course of the assay (Figure 3D).

Figure 4A plots CYP2C9 activity against time of incubation with a proprietary AstraZeneca compound, AZ1. AZ1 inhibited CYP2C9 mediated diclofenac 4'-hydroxylation in a time and concentration dependent manner from 0.1 to 10 μ M. CYP2C9 activity was not significantly inhibited by 0.1 μ M AZ1 but was effectively abolished by 24 h after incubation with 5 μ M AZ1. CYP1A2, 2C19, 2D6 and 3A4 activities were unaffected by the presence of up to 10 μ M AZ1. AZ1 concentration was determined throughout the time-course of the assay (Figure 4B).

Comparison of K_i and k_{inact} values from different enzyme sources

The kinetic constants of time-dependent inhibition, K_i and k_{inact} , were estimated in rCYPs for the inhibitor/CYP pair that demonstrated clear time-dependent inhibition in human hepatocytes. K_i and k_{inact} values were determined using rCYPs and HLM as described in

DMD#9969

Materials and Methods. Table 2 compares K_i and k_{inact} estimates generated in rCYPs and human hepatocytes with the relevant selective substrate, to data reported in the literature, using HLM or rCYPs as the enzyme source. Generally there is good agreement between values generated in this laboratory versus those reported in the literature. Mean values from triplicate rCYPs experiments were compared to K_i and k_{inact} estimates generated using mean human hepatocyte data shown in Figures 1, 3 and 4. The fraction unbound (f_{uinc}) of the inhibitors in the hepatocytes milieu were estimated from the method of Austin et al., 2005 and incorporated in the model to generate unbound K_i values (see Materials and Methods), allowing a direct comparison to values estimated from rCYP where, due to the very low protein level (<0.05 mg/ml), values approaching unbound K_i would be determined. Table 2 lists both *apparent* and *unbound* K_i values for fluoxetine in HLM, where f_{uinc} at 1 mg/ml HLM is 0.1 (Austin et al., 2002), which is of the same order as that determined experimentally (Margolis and Obach, 2003). All other inhibitors, being significantly less lipophilic than fluoxetine, have higher f_{uinc} and therefore apparent K_i approaches unbound K_i values.

Tienilic acid at CYP2C9 generated K_i and k_{inact} values from rCYP vs human hepatocytes of 2 μM & 0.19 min^{-1} vs 2 μM & 0.05 min^{-1} respectively; erythromycin/CYP3A4 9 μM & 0.12 min^{-1} vs 11 μM & 0.07 min^{-1} ; troleandomycin/CYP3A4 0.3 μM & 0.12 min^{-1} vs 0.4 μM & 0.05 min^{-1} and AZ1/CYP2C9 30 μM & 0.02 min^{-1} vs 19 μM & 0.02 min^{-1} . Therefore, for tienilic acid, erythromycin, troleandomycin and AZ1 there was good concordance of the kinetic constants between the rCYPs and human hepatocytes.

For fluoxetine, time-dependent inhibition in human hepatocytes was observed for both CYP3A4 and CYP2C19 mediated reactions. There was good agreement between unbound K_i and k_{inact} values generated using rCYP3A4 (2 μM & 0.03 min^{-1} respectively), HLM (0.5 μM (apparent K_i 5 μM) & 0.01 min^{-1}) and human hepatocytes (1 μM & 0.01 min^{-1}) for midazolam 1'-hydroxylation. The apparent K_i and k_{inact} values generated in HLM similarly agreed with those previously reported, 5 μM & 0.02 min^{-1} respectively (Mayhew et

DMD#9969

al., 2000). The time-dependent inhibition of rCYP2C19 by fluoxetine, using S-mephenytoin 4'-hydroxylation as the probe reaction, is shown in Figure 5. There was a reasonable agreement for the unbound K_i and k_{inact} values generated using HLM (0.8 μM (apparent K_i 8 μM) & 0.03 min^{-1}) and human hepatocytes (0.2 μM & 0.04 min^{-1}). Using rCYP2C19, the unbound K_i (0.4 μM) was similar to the HLM and hepatocytes values but the k_{inact} was significantly higher (0.5 min^{-1}) (Table 2). No time or NADPH dependent inhibition was observed with fluoxetine for rCYP2D6 in accordance with the lack of significant time dependency observed for fluoxetine/CYP2D6 in human hepatocytes (Figure 3C).

Discussion

Drug discovery departments in the pharmaceutical industry employ a battery of screens to assess the potential of new chemical entities to cause DDIs via CYP inhibition and induction. Recently, screens that identify mechanism-based, or more specifically time-dependent CYP inhibitors have been developed, in our laboratory (Atkinson et al., 2005) and others (Lim et al., 2005; Zhao et al., 2005). Such assays typically use HLMs or rCYPs as the enzyme source. More recently, cryopreserved human hepatocytes in suspension have been used to study the time-dependent inactivation of CYP3A (Zhao et al., 2005).

In this study, the impact of time-dependent CYP inhibition in primary cultures of human hepatocytes was evaluated using a cocktail of CYP substrates. Use of a substrate cocktail allows for the maximum amount of data to be retrieved from the limited resource of human hepatocytes (Mohutsky et al., 2005). CYP mRNA expression and catalytic activities are differentially expressed during human hepatocyte culture (LeCluyse, 2001). In this study the effect of compounds on CYP activity are relative to a solvent control at each time point, and so the observed inhibitory effect can be assumed to be exclusively as a result of the inhibitor and not compromised by any loss of CYP enzyme throughout the culture period.

An adaptation of the physiological based model developed by Ito et al., 2003 for predicting clinical mechanism-based DDIs, was used to describe the effect on CYP activities observed in primary culture by prototypic mechanism-based CYP inhibitors. K_i and k_{inact} values were estimated from non-linear regression analysis using Equations 2 and 4 with an estimate of inhibitor CL_{int} and CYP activity values determined from cultured human hepatocytes, and were compared with values obtained from rCYPs and HLM. In the absence of definitive K_{deg} values for individual CYPs in cultured human hepatocytes a value of 0.00025 min^{-1} was used for all CYPs, based on the turnover rate constant for CYP3A in cultured human hepatocytes (Pichard et al., 1992).

Tienilic acid is activated by human liver CYP2C9, to form reactive thiophene sulfoxides leading to CYP2C9 inactivation (Lopez-Garcia et al., 1994). The mean K_i and k_{inact} values

estimated from non-linear regression analysis of the human hepatocyte data using a selective CYP2C9 probe (K_i 2 μM and k_{inact} 0.05 min^{-1}) are in reasonable concordance with the values derived using rCYP2C9 (K_i 2 μM and k_{inact} 0.19 min^{-1}) (Table 2). In addition the fitted inactivation curves well describe the tienilic acid dependent CYP2C9 inhibition (Figure 1A).

The macrolide antibiotics erythromycin and troleandomycin are well-established mechanism-based inhibitors of CYP3A4 via reactive nitroso species derived heme complexes (Periti et al., 1992). Recently the time-dependent nature of CYP3A4 inhibition by erythromycin and troleandomycin in human hepatocytes has been reported (Zhao et al., 2005) and this has been reproduced in this study. The K_i and k_{inact} values estimated from human hepatocyte data using a selective CYP3A4 probe (erythromycin, K_i 11 μM & k_{inact} 0.07 min^{-1} ; troleandomycin, 0.4 μM & 0.05 min^{-1} respectively) are similar to those determined in rCYP3A4 (erythromycin, 9 μM & 0.12 min^{-1} ; troleandomycin, 0.3 μM & 0.12 min^{-1} respectively). The values generated are also comparable to several literature reports of K_i and k_{inact} estimates using rCYP3A4 and HLM (Table 2).

The fitted CYP3A4 inactivation curves for erythromycin and troleandomycin in human hepatocytes describe the initial degree of CYP3A4 inactivation reasonably well (Figure 1B and 1C). Although troleandomycin is a relatively potent time-dependent CYP3A4 inhibitor, it is rapidly cleared in cultured human hepatocytes, (CL_{int} values range from 37-51 $\mu\text{l}/\text{min}/10^6$ cells, Table 1 and Figure 1F) and the model simulates the recovery of CYP3A4 activity after 2-3 h, when essentially troleandomycin is removed from the incubation (Figure 1F). The rate of regain of activity, described by the model, is a function of the turnover or K_{deg} constant. This compares to erythromycin which, although a weaker CYP3A4 TDI inhibitor than troleandomycin (Table 2), is cleared more slowly (5-15 $\mu\text{l}/\text{min}/10^6$ cells, Figure 1E) and the CYP3A4 activity in human hepatocytes, is therefore, simulated to recover only after several hours into the incubation (Figure 1B). Tienilic acid is an example of a slowly cleared (5-9 $\mu\text{l}/\text{min}/10^6$ cells, Figure 1D), relatively potent, time-

dependent inhibitor of CYP2C9 (Table 2), which demonstrates no recovery of CYP2C9 activity over the 48 h of the incubation and is correctly simulated by the model (Figure 1A). The model assumes the CYP degradation rate is equal to the synthesis rate in cell culture for the duration of the experiment and describes activity recovery as a function of clearance of the irreversible inhibitor and synthesis of new protein. Of course the situation for some inhibitors is likely more complex than that described by the model, for example, both parent and any subsequently formed metabolites may be reversibly or irreversibly inhibitory to different extents towards the CYP. For both erythromycin and troleandomycin the model underestimates the degree of regain in activity up to 48 h (Figure 1B and 1C). This may also be explainable if the half-life of CYP3A4 in these cultured human hepatocytes is somewhat shorter than previously estimated ($k_{deg} = 0.00025 \text{ min}^{-1}$, $t_{1/2} = 46 \text{ h}$ (Pichard et al., 1992)) as demonstrated by the simulations for troleandomycin (Figure 2). Similarly the underestimation could be a result of up-regulation of CYP3A4 by the macrolide antibiotics. There are apparently conflicting literature reports regarding the effects of the macrolide antibiotics on CYP3A4 mRNA, protein and activity. Troleandomycin (20 μM) is a potent activator of hPXR in a reporter gene assay, but did not induce CYP3A4 mRNA, protein or activity in human hepatocytes (Luo et al., 2002; Faucette et al., 2004). However, several laboratories have reported moderately raised CYP3A4 protein levels using troleandomycin (Meunier et al., 2000; Johnson et al., 2005), associated with increased (Ledirac et al., 2000) or decreased CYP3A activity (Pichard et al., 1990). Similarly for erythromycin there are reports of the absence (Ledirac et al., 2000) and presence (Pichard et al., 1990) of CYP3A4 protein induction as determined by western blotting. In this laboratory we have demonstrated erythromycin and troleandomycin to be weak inducers of CYP3A4 as determined by RT-PCR and Western blotting (data not shown). Despite the lack of consensus, the macrolide antibiotics are likely to be weak CYP3A4 inducers and by using enzyme activity as the sole endpoint, time-dependent inhibition obfuscates a thorough assessment of their CYP mediated DDI potential.

Fluoxetine is moderately cleared in human hepatocytes with CL_{int} values ranging from 9-35 $\mu\text{l}/\text{min}/10^6$ cells (Table 1). Fluoxetine has been established as a mechanism-based inhibitor of CYP3A4 (Mayhew et al., 2000) and a potent yet *reversible* inhibitor of CYP2D6 (Bertelsen et al., 2003). The results in this study are consistent with these reports. Due to the high lipophilicity of fluoxetine (logP 4.1), it shows a significant degree of non-specific binding to HLM (Margolis and Obach, 2003) and hepatocytes under the experimental conditions used (Austin et al., 2002, 2005), much more so than the other inhibitors, where apparent K_i will approximate unbound K_i . The $f_{u,inc}$ value is an input to the hepatocyte model, allowing unbound K_i values to be estimated which are comparable to the unbound K_i values estimated in rCYP, where due to the low protein concentration $f_{u,inc}$ will approach unity. There was clear time-dependency of fluoxetine dependent CYP3A4 inhibition in human hepatocytes with inactivation curves for the 1 and 10 μM data described well using Equation 4 (Figure 3A). The CYP3A4 dependent K_i and k_{inact} values in human hepatocytes (6 μM & 0.01 min^{-1} respectively) are comparable to values determined in rCYP3A4 (2 μM & 0.03 min^{-1}) and HLM (5 μM & 0.01 min^{-1}) (Table 2). Fluoxetine at 1 and 10 μM showed significant inhibition of CYP2D6 mediated bufuralol 1'-hydroxylase activity but demonstrated only weak, if any, time-dependency, consistent with *reversible* CYP2D6 inhibition (Figure 3C).

Fluoxetine has been reported as an inhibitor of CYP2C19 mediated S-mephenytoin 4'-hydroxylase activity in HLM with a K_i of 5 μM (Kobayashi et al., 1995). The authors used Lineweaver-Burk analysis of S-mephenytoin 4'-hydroxylase inhibition at a single time point to conclude fluoxetine was acting competitively. However, any time-dependency to the inhibition would not be apparent from such an analysis. Data generated here, in human hepatocytes, strongly suggest that this interaction is time-dependent (Figure 3B). This was subsequently confirmed by experiments carried out in rCYP2C19 and HLM (Table 2, Figure 4). After consideration of non-specific binding, the unbound K_i in human hepatocytes (0.2 μM) was comparable to those determined in rCYP2C19 (0.4 μM) and

DMD#9969

HLM (0.8 μM , Table 2). Interestingly, the k_{inact} appears to be significantly higher when determined in rCYP2C19 (0.5 min^{-1}) compared to HLM and human hepatocytes (0.03 & 0.04 min^{-1} respectively). A similar phenomenon has been described with propranolol and CYP2D6, causing mechanism-based inhibition in rCYP but not CYP2D6 in HLM (Palamanda et al., 2005). Although the model accurately simulated the initial loss of CYP2C19 dependent activity in human hepatocytes at the two fluoxetine concentrations, the recovery of activity at 48 h (66% at 1 μM and 38% at 10 μM) was not predicted. Reasons for this CYP specific increase in activity (it was not observed for any of the remaining four CYPs studied) may include, the k_{deg} of CYP2C19 being significantly greater than the CYP3A value of 0.00025 min^{-1} , or possibly fluoxetine induces CYP2C19 in cultured human hepatocytes, analogous to the macrolide antibiotics effect on CYP3A4. Consistent with the *in vitro* interaction with CYP2C19, fluoxetine has been reported to significantly decrease the *in vivo* clearance of CYP2C19 substrates diazepam (Lemberger et al., 1988) and S-mephenytoin (Jeppesen et al., 1996; Harvey and Preskorn, 2001). The major human metabolite of fluoxetine, norfluoxetine, may also be responsible for CYP inhibition and this has not been addressed directly in the present studies; we have yet to examine whether norfluoxetine, which is equipotent against CYP2D6 (Stevens and Wrighton, 1993), shows time-dependent inhibition of CYP2C19 and 3A4. Moreover, as fluoxetine is a racemic mixture clearly there could be differences in the CYP3A4 and 2C19 interaction between the R and S form, as reported for CYP2D6 inhibition (Stevens and Wrighton, 1993). Fluoxetine has also been demonstrated to be a mechanism-based inhibitor of rat CYP2C11 (Murray and Murray, 2003).

Whilst assessing the potential of AZ1 to induce CYPs in cultured human hepatocytes, the compound was shown to cause significant loss of CYP2C9 mediated diclofenac 4'-hydroxylation, with minimal effect on CYP2C9 protein level as determined by Western blotting (data not shown). Prior to this, it had been established that AZ1 was not a potent time-dependent inhibitor of CYP2C9, using a recently described HLM assay (Atkinson et al., 2005). After further investigations at higher concentrations and longer time-points than

DMD#9969

would have been used in a standard screen, AZ1 was identified as an extremely weak CYP2C9 inhibitor. The $k_{\text{inact}}:K_i$ ratio (a measure of TDI efficiency) for AZ1, as determined in rCYP2C9, is 7×10^{-4} ml/ min. nmol (K_i 30 μM , k_{inact} 0.02 min^{-1} , Table 2) which is approximately 140 times smaller than that of tienilic acid (K_i 2 μM , k_{inact} 0.19 min^{-1} , $k_{\text{inact}}:K_i$ 0.1 ml/ min. nmol). Despite the relatively weak CYP2C9 TDI properties of AZ1, the inhibitory effect in cultured human hepatocytes was dramatic, due to the supra-pharmacological (free) compound concentrations used, the resultant “stoichiometry” of test compound to cells, the long time course involved (typically 72 h with compound replenished every 24 h) which is exacerbated by low turnover of inhibitor, an increasingly common property for candidate drugs for oral therapies where hepatic clearance is required to be low. Using a modified version of the physiological model developed by Ito et al., 2003 (Equation 4), CYP inhibition in cultured human hepatocytes can be quantitatively described. The original *in vitro-in vivo* model predicted accurately the two-fold AUC increase of intravenously dosed midazolam following pre-treatment with erythromycin (500 mg t.i.d.) (Ito et al., 2003) yet predicts minimal risk of significant CYP2C9 mediated clinical drug-drug interactions with a weak time-dependent inhibitor such as AZ1 (Figure 6). However, the suppression of CYP activity in hepatocytes indicated the potential for reactive metabolite formation and prompted further investigations such as covalent binding work, leading to a better risk assessment of immune-related hypersensitivity reactions in the clinic.

This study has confirmed the importance of considering time-dependent CYP inhibition whilst using primary hepatocytes for assessing CYP induction, as cautioned previously (Silva and Nicoll-Griffith, 2002). The effect on CYP activity of a time-dependent inhibitor depends on the interplay between the efficiency of inactivation caused by parent (and/or subsequently formed metabolites), the turnover rate of both parent and individual CYP, together with any CYP induction. Clearly, reversible inhibitors can be removed by thoroughly washing cells before determination of CYP activity. As exemplified by AZ1, relatively weak time-dependent inhibitors that are cleared slowly may show dramatic

DMD#9969

inhibitory effects on CYP activity in primary culture over hours and/or days, especially as compound is traditionally replenished every 24 h. These data are particularly relevant as many oral drug candidates will be relatively metabolically stable and some may demonstrate a degree of time-dependent CYP inhibition. Metabolically labile and/or potent time-dependent CYP inhibitors are likely to be eliminated from a lead-optimisation screening cascade before entering resource-intensive CYP induction assays.

In conclusion, cultured human hepatocytes provide a sensitive system for studying time-dependent CYP inhibition. Together with a CYP-selective substrate cassette approach, this provides an efficient assay that also flags the potential formation of reactive species and provides some indication of clinical toxicity risk. In order to fully evaluate the CYP induction potential of a drug candidate, mRNA and/or protein levels should be measured in addition to CYP activity, typically referred to as the 'gold standard' endpoint, particularly if detailed knowledge of time-dependent CYP inhibition potential is lacking.

DMD#9969

References

Atkinson A, Kenny JR, and Grime K (2005) Automated assessment of time-dependent inhibition of human cytochrome-P450 enzymes using liquid chromatography-tandem mass spectrometry analysis. *Drug Metab Dispos* **33**:1637-1647.

Austin RP, Barton P, Cockroft SL, Wenlock MC, and Riley RJ (2002) The influence of nonspecific microsomal binding on apparent intrinsic clearance, and its prediction from physicochemical properties. *Drug Metab Dispos* **30**:1497-1503.

Austin RP, Barton P, Mohamed S, and Riley RJ (2005) The binding of drugs to hepatocytes and its relationship to physicochemical properties. *Drug Metab Dispos* **33**:419-425.

Bertelsen KM, Venkatakrishnan K, von Moltke LL, Obach RS, and Greenblatt DJ (2003) Apparent mechanism-based inhibition of human CYP2D6 in vitro by paroxetine: Comparison with fluoxetine and quinidine. *Drug Metab Dispos* **31**:289-293.

Bertz RJ and Granneman GR (1997) Use of in vitro and in vivo data to estimate the likelihood of metabolic pharmacokinetic interactions. *Clin Pharmacokinet* **32**:210-258.

Chan WK and Delucchi AB (2000) Resveratrol, a red wine constituent, is a mechanism-based inactivator of cytochrome P450 3A4. *Life Sci* **67**:3103-3112.

Dai R, Wei X, Luo G, Sinz M, and Marathe P (2003) Metabolism-dependent P450 3A4 inactivation with multiple substrates. Abstract from 12th North American ISSX Meeting. Providence, RI. *Drug Metab Rev* **35**:341.

DMD#9969

Faucette SR, Wang H, Hamilton GA, Jolley SL, Gilbert D, Lindley C, Yan B, Negishi M, and LeCluyse EL (2004) Regulation of CYP2B6 in primary human hepatocytes by prototypical inducers. *Drug Metab Dispos* **32**:348-358.

Harvey AT and Preskorn SH (2001) Fluoxetine pharmacokinetics and effect on CYP2C19 in young and elderly volunteers. *J Clin Psychopharm* **21**:161-166.

Ito K, Ogihara K, Kanamitsu SI, and Itoh T (2003) Prediction of the in vivo interaction between midazolam and macrolides based on in vitro studies using human liver microsomes. *Drug Metab Dispos* **31**:945-954.

Jankel CA and Fitterman LK (1993) Epidemiology of drug-drug interactions as a cause of hospital admissions. *Drug Safety* **9**:51-59.

Jeppesen U, Gram LF, Vistisen K, Loft S, Poulsen HE, and Broesen K (1996) Dose-dependent inhibition of CYP1A2, CYP2C19 and CYP2D6 by citalopram, fluoxetine, fluvoxamine and paroxetine. *Eur J Clin Pharmacol* **51**:73-78.

Johnson JA, Creighton TP, Chandler C, Crespi CL, and Stresser DM (2005) Validation of a cytochrome P450 induction assay using microsomes prepared from primary cultures of human hepatocytes. Abstract from 13th North American ISSX Meeting. Maui, Hawaii. *Drug Metab Rev* **37**(Suppl 2):151.

Kanamitsu S, Ito K, Green CE, Tyson CA, Shimada N, and Sugiyama Y (2000) Prediction of in vivo interaction between triazolam and erythromycin based on in vitro studies using human liver microsomes and recombinant human CYP3A4. *Pharm Res* **17**:419-426.

DMD#9969

Kato M, Chiba K, Horikawa M, and Sugiyama Y (2005) The quantitative prediction of in vivo enzyme-induction caused by drug exposure from in vitro information on human hepatocytes. *Drug Metab Pharmacokinet* **20**:236-243.

Kobayashi K, Yamamoto T, Chiba K, Tani M, Ishizaki T, and Kuroiwa Y (1995) The effects of selective serotonin reuptake inhibitors and their metabolites on S-mephenytoin 4'-hydroxylase activity in human liver microsomes. *Br J Clin Pharmacol* **40**:481-485.

Larrey D, Tinel M, and Pessayre D (1983) Formation of inactive cytochrome P-450 Fe(II)-metabolite complexes with several erythromycin derivatives but not with josamycin and midecamycin in rats. *Biochem.Pharmacol* **32**:1487-1493.

LeCluyse EL (2001) Human hepatocyte culture systems for the in vitro evaluation of cytochrome P450 expression and regulation. *Eur J Pharm Sci* **13**:343-368.

LeCluyse E, Madan A, Hamilton G, Carroll K, DeHaan R, and Parkinson A (2000) Expression and regulation of cytochrome P450 enzymes in primary cultures of human hepatocytes. *J Biochem Mol Toxicol* **14**:177-188.

Ledirac N, de Sousa G, Fontaine F, Agouridas C, Gugenheim J, Lorenzon G, and Rahmani R (2000) Effects of macrolide antibiotics on CYP3A expression in human and rat hepatocytes: interspecies differences in response to troleandomycin. *Drug Metab Dispos* **28**:1391-1393.

Lemberger L, Rowe H, Bosomworth JC, Tenbarger JB, and Bergstrom RF (1988) The effect of fluoxetine on the pharmacokinetics and psychomotor responses of diazepam. *Clin Pharmacol Ther* **43**:412-419.

Lim HK, Duczak N, Jr., Brougham L, Elliot M, Patel K, and Chan K (2005) Automated screening with confirmation of mechanism-based inactivation of CYP3A4, CYP2C9, CYP2C19, CYP2D6, and CYP1A2 in pooled human liver microsomes. *Drug Metab Dispos* **33**:1211-1219.

Lopez-Garcia MP, Dansette PM, and Mansuy D (1994) Thiophene derivatives as new mechanism-based inhibitors of cytochromes P-450: inactivation of yeast-expressed human liver cytochrome P-450 2C9 by tienilic acid. *Biochemistry* **33**:166-175.

Luo G, Cunningham M, Kim S, Burn T, Lin J, Sinz M, Hamilton G, Rizzo C, Jolley S, Gilbert D, Downey A, Mudra D, Graham R, Carroll K, Xie J, Madan A, Parkinson A, Christ D, Selling B, LeCluyse E, and Gan LS (2002) CYP3A4 induction by drugs: correlation between a pregnane X receptor reporter gene assay and CYP3A4 expression in human hepatocytes. *Drug Metab Dispos* **30**:795-804.

Luo G, Guenther T, Gan LS, and Humphreys WG (2004) CYP3A4 induction by xenobiotics: biochemistry, experimental methods and impact on drug discovery and development. *Curr Drug Metab* **5**:483-505.

Margolis JM and Obach RS (2003) Impact of nonspecific binding to microsomes and phospholipid on the inhibition of cytochrome P450 2D6: Implications for relating in vitro inhibition data to in vivo drug interactions. *Drug Metab Dispos* **31**:606-611.

Mayhew BS, Jones DR, and Hall SD (2000) An in vitro model for predicting in vivo inhibition of cytochrome P450 3A4 by metabolic intermediate complex formation. *Drug Metab Dispos* **28**:1031-1037.

DMD#9969

McConn DJ, II, Lin YS, Allen K, Kunze KL, and Thummel KE (2004) Differences in the inhibition of cytochromes P450 3A4 and 3A5 by metabolite-inhibitor complex-forming drugs. *Drug Metab Dispos* **32**:1083-1091.

McGinnity DF, Tucker J, Trigg S, and Riley RJ (2005) Prediction of CYP2C9 mediated drug-drug interactions: a comparison using data from recombinant enzymes and human hepatocytes. *Drug Metab Dispos* **33**:1700-1707.

McGinnity DF, Soars MG, Urbanowicz RA, and Riley RJ. (2004) Evaluation of fresh and cryopreserved hepatocytes as in vitro drug metabolism tools for the prediction of metabolic clearance. *Drug Metab Dispos* **32**:1247-1253.

Meunier V, Bourrie M, Julian B, Marti E, Guillou F, Berger Y, and Fabre G (2000) Expression and induction of CYP1A1/1A2, CYP2A6 and CYP3A4 in primary cultures of human hepatocytes: a 10-year follow-up. *Xenobiotica* **30**:589-607.

Mohutsky MA, Petullo DM, and Wrighton SA (2005) The use of a substrate cassette strategy to improve the capacity and throughput of cytochrome P450 induction studies in human hepatocytes. *Drug Metab Dispos* **33**:920-923.

Murray M and Murray K (2003) Mechanism-based inhibition of CYP activities in rat liver by fluoxetine and structurally similar alkylamines. *Xenobiotica* **33**:973-987.

Palamanda, Jairam R., Kumari, P., Kim, H., and Nomeir, A. A. (2005) Mechanism-Based inhibition of recombinant CYP2D6 but not human liver microsomal CYP2D6 by propranolol. Abstract from 13th North American ISSX Meeting. Maui, Hawaii. *Drug Metab Rev* **37**(Suppl 2):257.

DMD#9969

Periti P, Mazzei T, Mini E, and Novelli A (1992) Pharmacokinetic drug interactions of macrolides. *Clin Pharmacokinet* **23**:106-131.

Pichard L, Fabre I, Daujat M, Domergue J, Joyeux H, and Maurel P (1992) Effect of corticosteroids on the expression of cytochromes P450 and on cyclosporin A oxidase activity in primary cultures of human hepatocytes. *Mol Pharmacol* **41**:1047-1055.

Pichard L, Fabre I, Fabre G, Domergue J, Saint AB, Mourad G, and Maurel P (1990) Cyclosporin A drug interactions. Screening for inducers and inhibitors of cytochrome P-450 (cyclosporin A oxidase) in primary cultures of human hepatocytes and in liver microsomes. *Drug Metab Dispos* **18**:595-606.

Ring BJ, Patterson BE, Mitchell MI, Vandenbranden M, Gillespie J, Bedding AW, Jewell H, Payne CD, Fogue ST, Eckstein J, Wrighton SA, and Phillips DL (2005) Effect of tadalafil on cytochrome P450 3A4-mediated clearance: studies in vitro and in vivo. *Clin Pharmacol Ther* **77**:63-75.

Silva JM and Nicoll-Griffith DA (2002) In vitro models for studying induction of cytochrome P450 enzymes, in *Drug-Drug Interactions* (Rodrigues AD ed) 189-216, Marcel Dekker, Inc., New York.

Silverman RB (1998) *Mechanism-Based Enzyme Inactivation: Chemistry and Enzymology*. Vol. I. CRC Press, Boca Raton, FL.

Stevens JC and Wrighton SA (1993) Interaction of the enantiomers of fluoxetine and norfluoxetine with human liver cytochromes P450. *J Pharmacol Exp Ther* **266**:964-971.

DMD#9969

Wang YH, Jones DR, and Hall SD (2004) Prediction of cytochrome P450 3A inhibition by verapamil enantiomers and their metabolites. *Drug Metab Dispos* **32**:259-266.

Weaver R, Graham KS, Beattie IG, and Riley RJ (2003) Cytochrome P450 inhibition using recombinant proteins and mass spectrometry/multiple reaction monitoring technology in a cassette incubation. *Drug Metab Dispos* **31**:955-966.

Yamano K, Yamamoto K, Katashima M, Kotaki H, Takedomi S, Matsuo H, Ohtani H, Sawada Y, and Iga T (2001) Prediction of midazolam CYP3A inhibitors interaction in the human liver from in vivo/in vitro absorption, distribution, and metabolism data. *Drug Metab Dispos* **29**:443-452.

Zhao P, Kunze KL, and Lee CA (2005) Evaluation of time-dependent inactivation of cyp3a in cryopreserved human hepatocytes. *Drug Metab Dispos* **33**:853-861.

Zhou S, Yung CS, Cher GB, Chan E, Duan W, Huang M, and McLeod HL (2005) Mechanism-based inhibition of cytochrome P450 3A4 by therapeutic drugs. *Clin Pharmacokinet* **44**:279-304.

DMD#9969

Footnotes

Send reprints to Dr. Dermot McGinnity, Department of Physical & Metabolic Science,
AstraZeneca R&D Charnwood, Bakewell Road, Loughborough, Leicestershire. LE11 5RH.
U.K.

Legends for Figures

Figure 1. CYP activity in cultured human hepatocytes after incubation with tienilic acid, erythromycin and troleandomycin

Using cultured human hepatocytes, CYP2C9 dependent diclofenac 4'-hydroxylation after incubation with tienilic acid (A), and CYP3A4-dependant midazolam 1'-hydroxylation after incubation with erythromycin (B) and troleandomycin (C) was determined as described in Materials and Methods. Data points represent the mean activity relative to a solvent control incubation (in the absence of inhibitor) at the corresponding time point from Donors 1, 3 and 5 for tienilic acid, and donors 1, 2, 4 and 5 for erythromycin and troleandomycin. Where activities from at least three donors were measured, error bars reflect the standard deviation from the mean. Closed and open circles indicate incubation with 1 μ M and 10 μ M inhibitor respectively. The solid and dashed lines indicate non-linear regression of the 1 and 10 μ M inhibitor data respectively, using equation 4 as described in Materials and Methods. Open squares represent the mean concentration of tienilic acid (D), erythromycin (E) and troleandomycin (F), from the 1 and 10 μ M incubations, over the time course of the experiment as determined by HPLC-MS/MS.

Figure 2. Simulation of CYP activity in cultured human hepatocytes after incubation with troleandomycin using three different CYP3A4 turnover rate constants

Data points represent the mean CYP3A4-dependant midazolam 1'-hydroxylation activity, relative to a solvent control incubation at the corresponding time point, after incubation with 1 μ M (closed circles) and 10 μ M (open circles) troleandomycin as shown in Figure 1C. The solid and dashed lines indicate non-linear regression of the 1 and 10 μ M inhibitor

DMD#9969

data respectively, using equation 4 with k_{deg} of A. 0.00025 min^{-1} , B. 0.0005 min^{-1} and C. 0.00075 min^{-1} .

Figure 3. CYP3A4, 2C19 and 2D6 activity in cultured human hepatocytes after incubation with fluoxetine.

Using cultured human hepatocytes, CYP3A4-dependent midazolam 1'-hydroxylation (A), CYP2C19 dependent S-mephenytoin 4'-hydroxylation (B) and CYP2D6 dependent bufuralol 1'-hydroxylation (C) was determined after incubation with $1 \mu\text{M}$ (closed circles) and $10 \mu\text{M}$ (open circles) fluoxetine, as described in Materials and Methods. Data points represent the mean activity relative to a solvent control incubation at the corresponding time point, from Donors 1, 3 and 5. Where activities from at least three donors were measured, error bars reflect the standard deviation from the mean. The solid and dashed lines indicate non-linear regression of the 1 and $10 \mu\text{M}$ fluoxetine data respectively, using equation 4, as described in Materials and Methods. Open squares represent the mean concentrations of fluoxetine (D) from the 1 and $10 \mu\text{M}$ incubations over the time course of the experiment as determined by HPLC-MS/MS.

Figure 4. CYP2C9 activity in cultured human hepatocytes after incubation with AZ1.

CYP2C9 dependent diclofenac 4'-hydroxylation after incubation with AZ1 was determined after incubation with $0.1 \mu\text{M}$ (closed squares), $1 \mu\text{M}$ (closed circles), $5 \mu\text{M}$ (closed triangles) and $10 \mu\text{M}$ (open circles) AZ1, as described in Materials and Methods. Data points represent the mean activity relative to a solvent control incubation at the corresponding time point, from Donors 3 and 5. The dash-dot, solid, dotted and dashed

DMD#9969

lines indicate non-linear regression of the 0.1, 1, 5 and 10 μM AZ1 data respectively, using equation 4, as described in Materials and Methods. Open squares represent the mean concentrations of AZ1 (B) from the 0.1, 1, 5 and 10 μM incubations over the time course of the experiment as determined by HPLC-MS/MS.

Figure 5. Time-dependent inhibition of rCYP2C19 by fluoxetine

The data were generated using S-mephenytoin 4'-hydroxylation in rCYP2C19 as described in Materials and Methods. A. The natural log of the % control activity remaining following incubation with increasing fluoxetine concentrations was plotted against the pre-incubation time. B. The slopes, k (inactivation rate constant) together with the fluoxetine concentration were used to determine K_i and k_{inact} by nonlinear regression analysis, using $k = k_{\text{inact}} \cdot I / (I + K_i)$. Each data point represents the mean from separate four experiments and error bars reflect the mean standard error.

Figure 6. Simulated profiles of CYP activity in human liver after oral dosing with AZ1 and erythromycin respectively.

Using the methodology of Ito et al., 2003, CYP2C9 activity in human liver was simulated after oral dosing with AZ1 (70 mg every 24 h for 72 h- open circles) and CYP3A4 activity in human liver after oral dosing with erythromycin (500 mg every 8 h for 72 h- closed circles). Physiological constants and the pharmacokinetic parameters of erythromycin needed for the simulation were taken directly from Ito et al., 2003 and are listed in Materials and Methods for AZ1.

DMD#9969

Table 1 CL_{int} values of inhibitors determined in five human hepatocyte donors.

Assays were carried out 12-16 h after plating and CL_{int} values determined by the rate of parent disappearance over 90 min as described in Materials and Methods. Final concentration of compounds was 1 μM. Due to limited numbers of hepatocytes all compounds were not incubated in all donors.

Compound	CL _{int} μl/min/10 ⁶ cells				
	Donor 1	Donor 2	Donor 3	Donor 4	Donor 5
Tienilic acid	5	7	6	7	9
Erythromycin	15	7	nd	nd	5
Troleandomycin	49	51	nd	nd	37
Fluoxetine	13	nd	35	10	9
AZ1	0.3	nd	0.3	nd	0.2

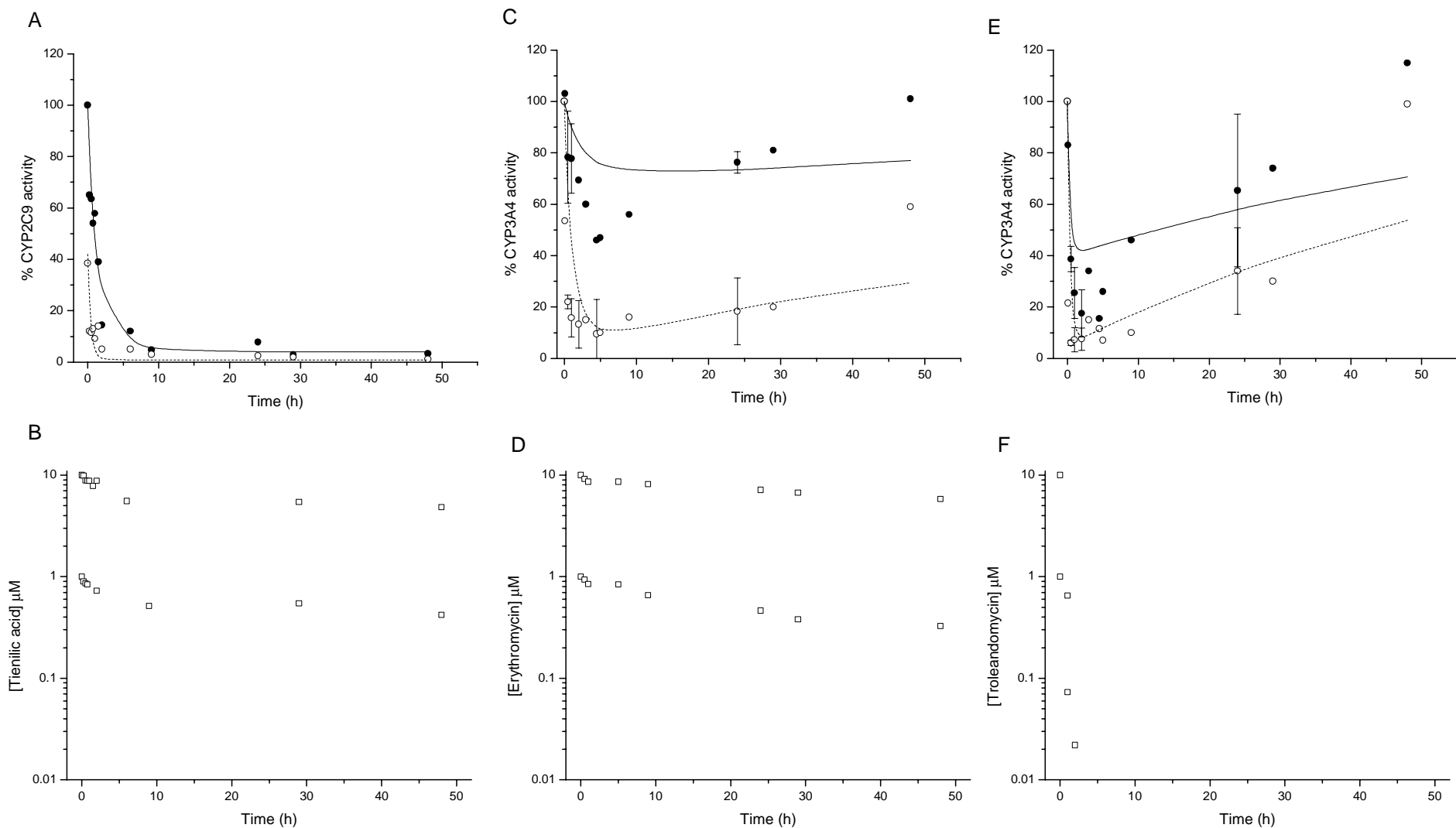
nd not determined

Table 2. Kinetic parameters of time-dependent inhibitors in different *in vitro* matrices

Compound	CYP Isoform	Enzyme Source	K_i (μM)	k_{inact} (min^{-1})	Reference
Tienilic acid	CYP2C9	rCYP2C9	2	0.19	This laboratory
		rCYP2C9 (2C10)	4	0.20	(Lopez-Garcia et al., 1994)
		Human hepatocytes	2	0.05	This laboratory
Erythromycin	CYP3A4	rCYP3A4	9	0.12	This laboratory (Atkinson et al., 2005)
		rCYP3A4	5	0.12	(Chan and Delucchi, 2000)
		HLM	16 ^a	0.07	(Kanamitsu et al., 2000)
		HLM	82 ^a	0.07	(Yamano et al., 2001)
		HLM	13 ^a	0.02	(Ito et al., 2003)
		HLM	10 ^a	0.08	(Dai et al., 2003)
		HLM	11 ^a	0.05	(McConn et al., 2004)
		HLM	15 ^a	0.07	(Zhao et al., 2005)
Troleandomycin	CYP3A4	Human hepatocytes	11	0.07	This laboratory
		rCYP3A4	0.3	0.12	This laboratory (Atkinson et al., 2005)
		rCYP3A4	0.2	0.15	(Chan and Delucchi, 2000)
		HLM	2 ^a	0.03	(Zhao et al., 2005)
Fluoxetine	CYP3A4	Human hepatocytes	0.4	0.05	This laboratory
		rCYP3A4	2	0.03	This laboratory
		HLM	5 ^a (0.5)	0.01	This laboratory
		HLM	5 ^a	0.02	(Mayhew et al., 2000)
		Human hepatocytes	1	0.01	This laboratory
		rCYP2C19	0.4	0.5	This laboratory
AZ1	CYP2C9	CYP2C19	8 ^a (0.8)	0.03	This laboratory
		Human hepatocytes	0.2	0.04	This laboratory
		rCYP2C9	30	0.02	This laboratory
		Human hepatocytes	19	0.02	This laboratory

^a *apparent* K_i values. All other values including those in parentheses are *unbound* K_i estimates

Figure 1



DMD Fast Forward. Published on May 5, 2006 as DOI: 10.1124/dmd.106.009699
This article has not been copyedited and formatted. The final version may differ from this version.

Figure 2

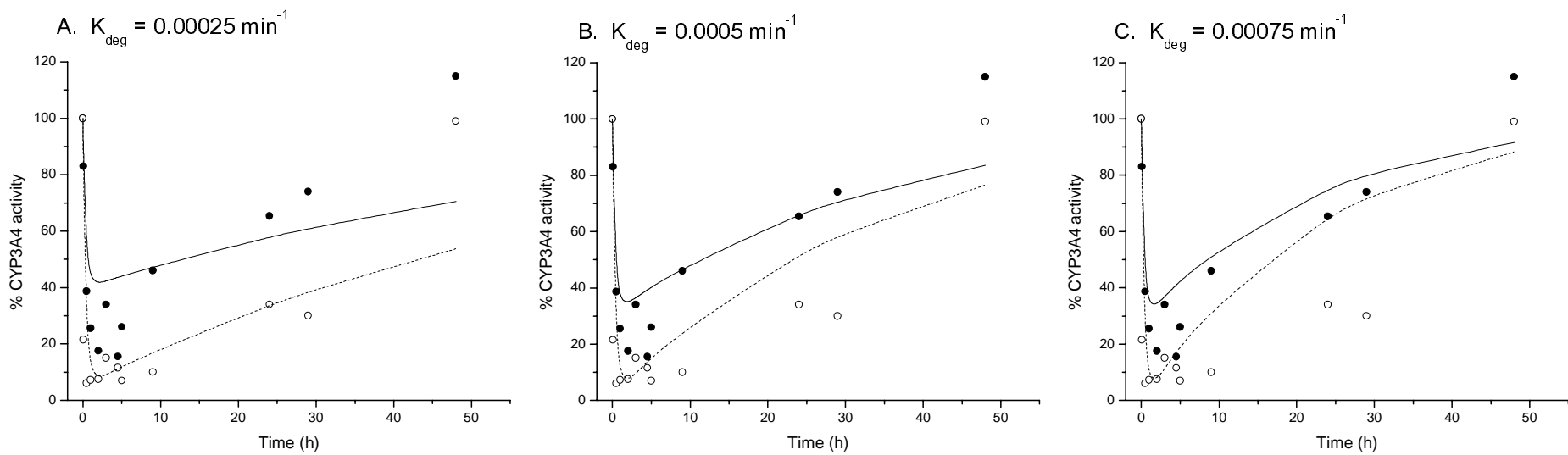


Figure 3

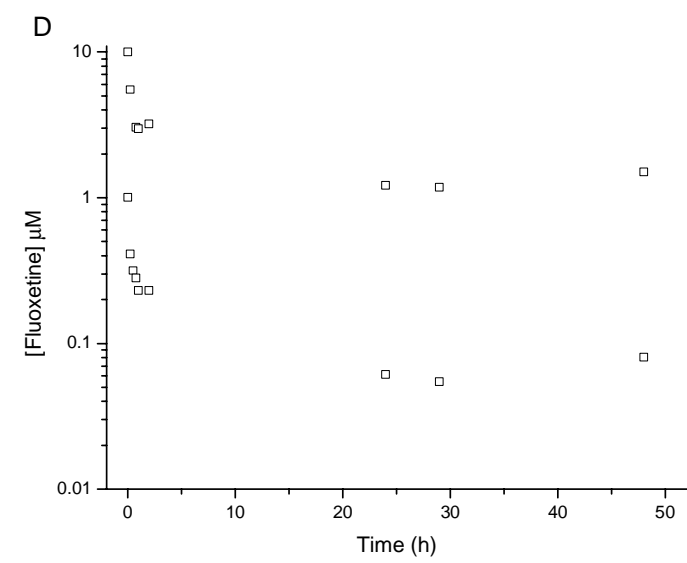
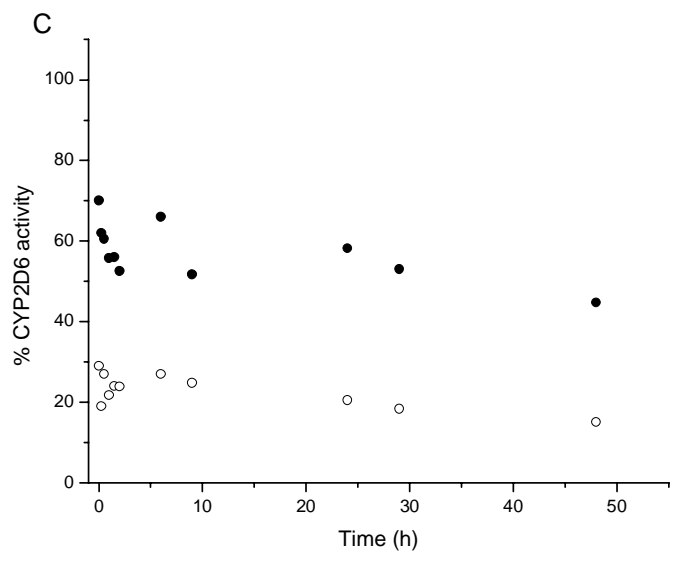
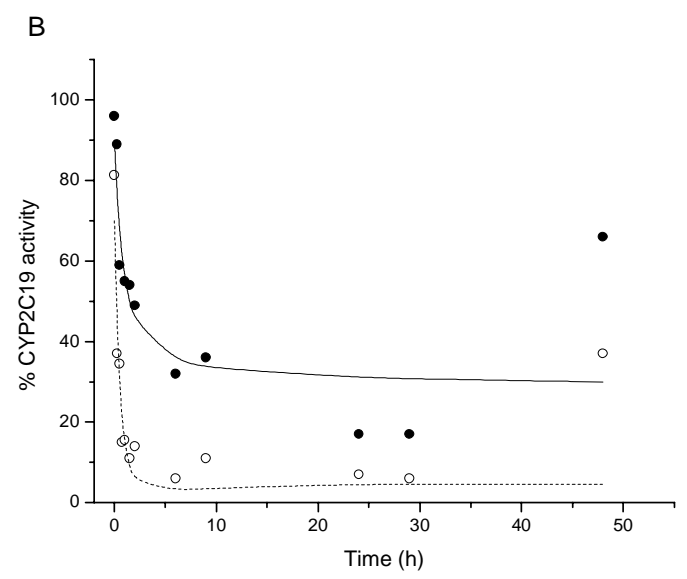
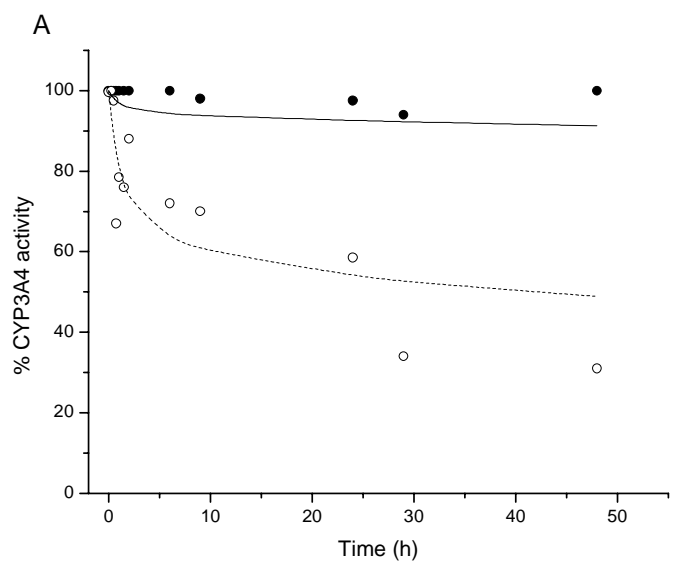


Figure 4

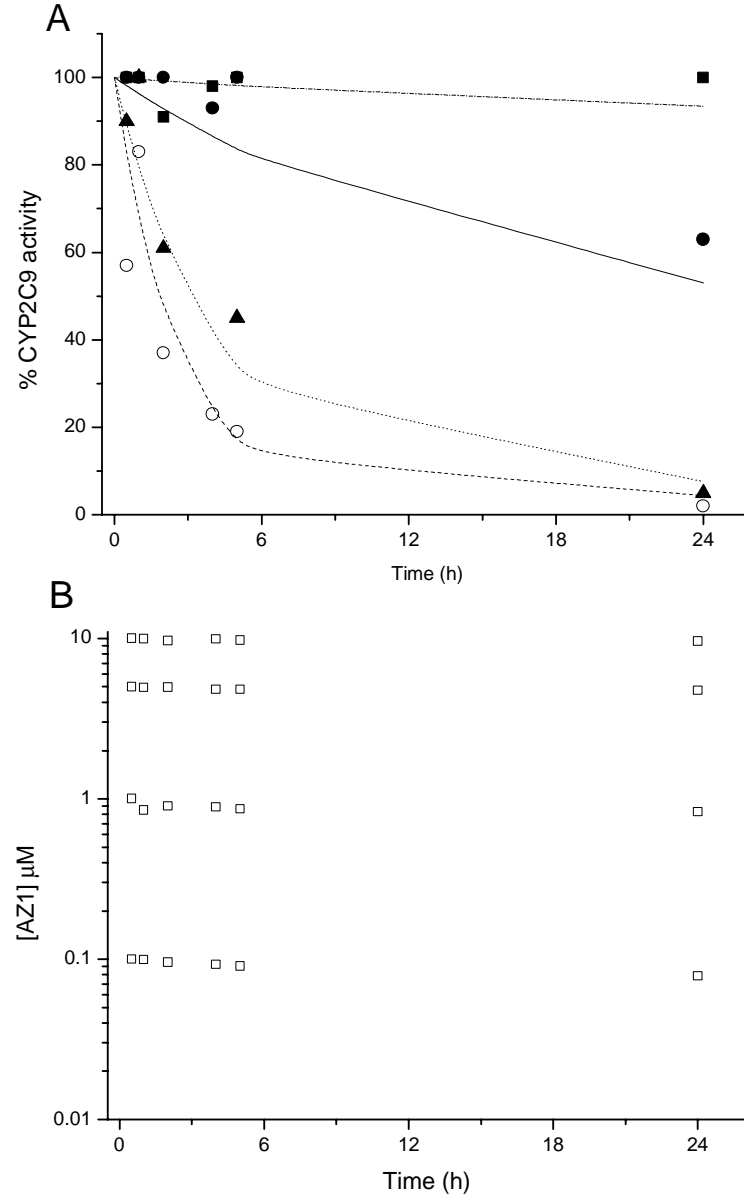


Figure 5

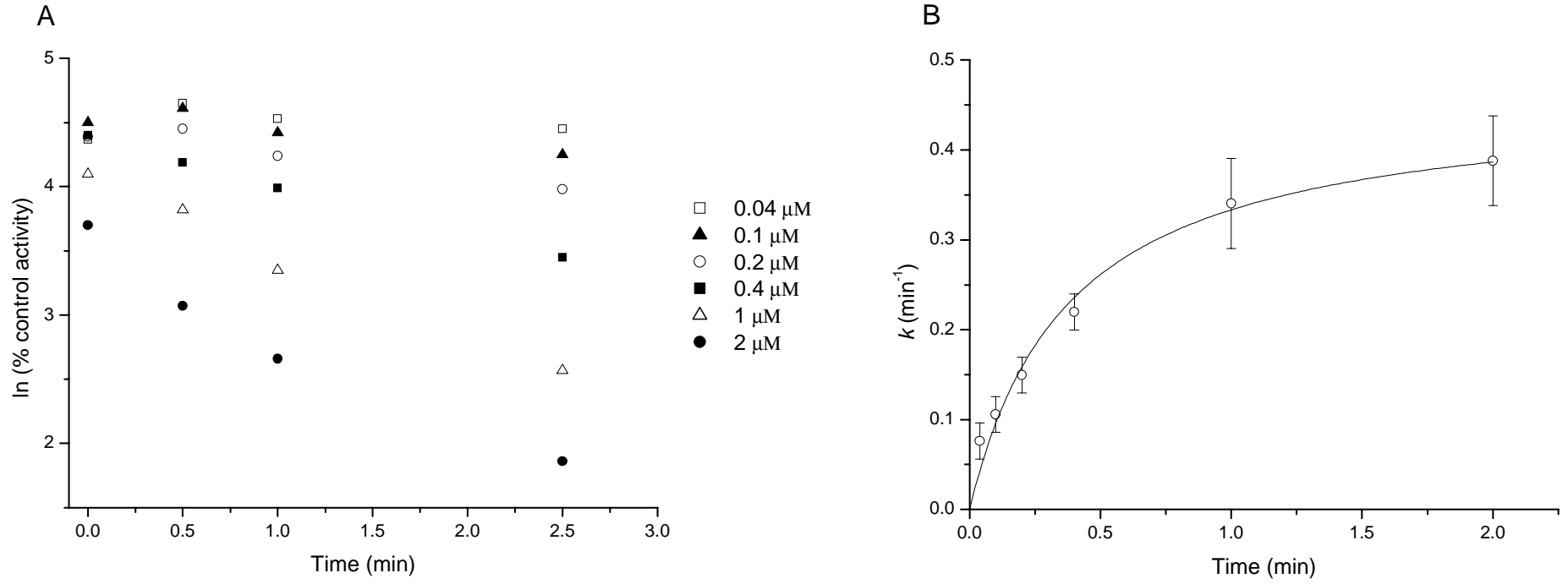


Figure 6

